

A Computational Parameter Study of Embryo Transfer

ISTVAN G. LAUKO,¹ PAOLO RINAUDO,² and SAVA DASHEV¹

¹Department of Mathematical Sciences, University of Wisconsin–Milwaukee, P.O. Box 413 Milwaukee, WI 53201-0413, USA
and ²Reproductive Endocrinology and Infertility, University of California–San Francisco, 2356 Sutter Street, 7th Floor,
San Francisco, CA 94115, USA

(Received 6 September 2006; accepted 9 January 2007; published online 8 February 2007)

Abstract—Embryo transfer (ET) is the final component of the in vitro fertilization process, and the limiting component to its success rate. The procedure is characterized by considerable technical variations in clinical practice and the effects of these different variations on the overall outcome is little understood. In this article we simulate the embryo transfer procedure based on a 2-dimensional fluid dynamics model and, in a large computational effort, we investigate the sensitivity of embryo placement on an array of procedural parameters. The results support the consensus among practitioners in what is the best choice of procedural factors. Based on the study we propose a set of optimal parameters with which to perform the ET procedure; in addition we suggest a novel technique of volume replacement prior to the catheter withdrawal.

Keywords—Embryo implantation, Uterine transport, Fluid dynamics simulation, Catheter volume replacement, In vitro fertilization.

INTRODUCTION

Embryo transfer (ET) refers to the final stage of the in vitro fertilization (IVF) process in which human embryos, placed in a liquid medium and loaded in a catheter, are injected into the uterine cavity. Normally 1–5 embryos are transferred, depending on the patient's age and medical history. Most frequently, embryos are transferred after 3 days in culture, but earlier or later transfers are possible (in the range of 2–5 days after fertilization). While real-time ultrasound imaging has been used lately to improve the effectiveness of ET (e.g., Ref. 12), the procedure essentially has not changed since its introduction and still is one of the limiting factors in the effectiveness of IVF.⁷ The implantation rate (the ratio of the number of embryos implanted and the embryos transferred)

varies according to the patient diagnosis, the patient age and the day of the transfer; even in the best case scenario, when transferring high quality embryo the implantation rate is not better than 65%.¹ Assuming that uterine receptivity, genetics, and unknown causes of implantation failure account for a portion of the failure rate per embryo (over 35%), the variability in efficiency of embryo transfer is high. Therefore, methods to improve the effectiveness of ET are needed.

The objective of ET is to place the non-motile embryo(s) in proximity of the uterine fundus while avoiding placement close to the fallopian tubes, a condition that could lead to ectopic pregnancy. There have been a number of clinical retrospective studies performed to evaluate the importance of such factors in ET as the chosen catheter type, catheter loading, the catheter's tip placement relative to the uterine fundus during injection, the injected fluid volume and the withdrawal of catheter.^{12,4,5,9,6,1}

Other potentially important factors such as the injection speed, the time window between the end of the injection stage and the catheter withdrawal and the withdrawal speed may also have an effect on the outcome of the transfer procedure.

Currently in clinical setting the speed of the injection is not controlled and the decision on how fast to inject the embryos is left to the experience and judgment of the skilled practitioner. It is generally accepted that a gentle procedure will avoid the onset of irregular uterine contractions. Uterine contractions are associated with lower implantation rates and possibly with higher incidence of ectopic pregnancies.⁵ It has also been observed that maintaining a low transfer fluid volume (in the 20–40 μ l range) improves the implantation rates. It appears that the underlying dynamics of the transfer is complex, highly dependent on the procedural parameters and the patients uterine anatomy; the relationship among all these factors are not well understood. For clarity we point out that the embryo is immotile *per se* and its changes in position are

Address correspondence to Istvan G. Lauko, Department of Mathematical Sciences, University of Wisconsin–Milwaukee, P.O. Box 413 Milwaukee, WI 53201-0413, USA. Electronic mail: igitlauko@uwm.edu

secondary to uterine contractions or to the movements of the flagella of the tubal cells.

Recently simulation studies on the biofluidmechanics aspects of ET have been reported in the literature, both on numerical simulation⁷ and in vitro experimental investigation.⁴

Eytan *et al.*⁴ have built a rigid, 2-dimensional uterine model to collect and analyze video information on the spread of colored transferred liquid from performed mock ET injection experiments. In Ref. 4 the effects of varying the transferred volume and the use of air or different viscosity fluids in the transferred material have been studied. The study did not consider the influence of either the injection speed, catheter tip placement or the catheter withdrawal on the embryo placement. The authors concluded that replacing air by fluid in the transferred medium may improve the implantation rates.³

Recent years have seen increased interest in biofluid computations in general and biofluidmechanics of reproduction in particular. For a comprehensive overview of published results see Ref. 8.

Yaniv *et al.*⁷ were the first to publish computed fluid dynamics simulations of ET. They investigated the effects of uterine peristalsis on ET during and after ET injection. They used a 2-dimensional model of a thin rectangular domain modified with sinusoidal waves superimposed on the side walls, traveling in time, to simulate injection in a sagittal uterine cross section. Their simulation, limited to the sagittal cross section, predicts that peristaltic oscillations of the uterine wall will only influence the axial transport during injection if the injection speed is low. The performed computational experiment suggests that higher injection velocity transports the embryo farther toward the fundus in the uterine cavity. The authors remarked on the shortcomings of the 2D sagittal model i.e., the fact that the widening of the uterine cavity in the missing lateral dimension likely influences the axial transport. Extension of the simulation in the missing lateral dimension may also be important to evaluate the possibility of transporting embryos towards the fallopian tubes that may increase the chances of ectopic pregnancies.

As it is suggested by the current body of literature fluid dynamics simulations may become important tools in the search for understanding the role of different procedural factors in improving the success rate of embryo transfer. Furthermore, since the anatomy/geometry of the uterine cavity (presence of fibroids and other deformations) is also thought to be an important factor in the procedure, simulation tools may eventually lead to the individualization of the procedure, i.e., the optimal adjustment of procedural factors for the individual patient.

In the present paper, we report on a numerical investigation of ET based on a 2-dimensional lateral uterus cross section model. Such a model allows us to investigate computationally the fluid dynamics effects on the particle transport, in the presence of the lateral dimension, that is missing in the simulations in Ref. 7. We obtained computational solutions of the incompressible Navier–Stokes equations to simulate ET on the lateral cross section uterine model including the three stages of the procedure such as injection, rest period and catheter withdrawal. Our objective was to develop a computational simulation tool that we can use to evaluate, quantitatively as well as qualitatively, the effects of a full array of ET procedural parameters on the embryo placement.

We performed parameter sensitivity studies on the simulated transfers assuming 6 independent procedural parameters, formulated a risk function to quantify the likelihood of successful implantation based on the fluid simulations and identified low risk parametric regions in the 6-dimensional parameter space.

Motivated by the observed dynamics in the performed simulations, among the 6 procedural parameters we included the novel procedural element of catheter volume replacement during the withdrawal stage, achieved by simultaneous additional fluid injection. This technique is aimed at limiting the withdrawal of the embryo toward the cervix during catheter removal and is not present in the current practice of ET. Not all the procedural parameters of ET can currently be controlled tightly, and to fully evaluate the predictions of our parameter study in clinical setting requires the design and introduction of a device for the control of injection flow rates and catheter removal.

To our knowledge, this is the most extensive computational study to date that examines the human embryo transfer procedure.

METHODS

Model Description

Embryo transfer is a mechanical procedure that involves the injection of a small fluid volume into the 3-dimensional uterine cavity. The cavity is often referred to as a virtual cavity, varying with the subject's anatomy; it is approximately an inverted equilateral triangle in an anterior-posterior oblique cross section, of height 6–9 cm, with its tip associated with the cervix area, and of a 3–3.5 cm long base, corresponding to the fundus. (For representation purposes we rotate this triangle by 90 degrees as shown on Figs. 1 and 2, and in this view we refer to the height as length and to the base

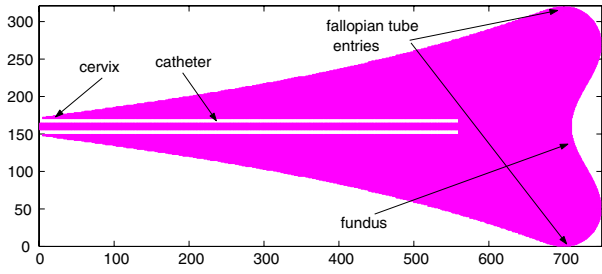


FIGURE 1. A 2D model of a 7.5 cm by 3.2 cm uterus with a catheter inserted. The shaded area represents the time dependent domain Ω_t where fluid motion is calculated.

as height.) It is also assumed that the uterine cavity contains a minimal amount of physiologic fluid, with the same density and viscosity of other bodily fluids. The viscosity of the human uterine fluid is not known. It is assumed in the literature that the value is approximately 1000 centipoise based on rheological studies of the uterine fluid of other mammals.² The size of the considered cavity, in any direction is under 10 cm. Initial simulations show that the value of the maximum speed does not exceed 10 cm/s. Using the assumption that the density of the fluid is approximately $\delta = 1$ g/cc the Reynolds number

$$Re = \frac{\delta_{\infty} u_{\infty} L}{\mu}$$

is approximately 10. In the orthogonal sagittal cross section the cavity is only approximately 1 mm deep, thus for fluid dynamics simulation purposes 2-dimensional fluid flow in the anterior-posterior cross section represents the injection flow dynamics well. Since fluid transport depends significantly on the domain geometry we made an effort to model the uterine cross section realistically, guided by ultrasound clinical images.

The domain with a smooth boundary that we used to represent the uterine cavity in our computations is an alteration of the triangular domain (of 7.5 cm length and 3.2 cm height) to a symmetric concave shape both on the sides and the base using cubic and sinusoidal correcting terms, respectively, and with connecting elliptic curves, with specified large and small axes in the vertex areas on the base. Specifically, the top side of the domain is given by correcting the AB line segment on Fig. 2 with the cubic term

$$Q(x) = \frac{c x^3}{d^3} - \frac{c x}{d}.$$

Here the variable x denotes distance variable in the horizontal (or axial) direction, the parameter d equals the length of the AB line section on Fig. 2 and the parameter c is related to the magnitude of the correction. On the fundus an indentation is produced by correcting the DE line segment on Fig. 2 with a full period

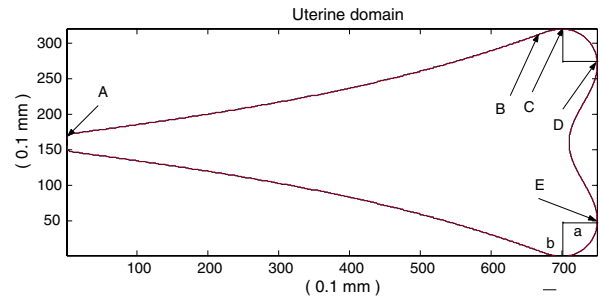


FIGURE 2. Construction of the 2D synthetic uterine model from simple, smoothly connecting curve sections.

sinusoidal wave of period DE length and specified amplitude m . These two curves are connected by the BD ellipse section of major and minor axes $2a$ and $2b$, respectively (See Fig. 2). The point B (and thus the parameter d) can be determined either analytically or numerically to ensure a smooth boundary curve. The point C in Fig. 2 is the assumed entry point of a fallopian tube. The specific values for the geometric parameters above (if distance is measured in cm) are $a = 0.50$, $b = 0.40$, $c = 0.42$ and $m = 0.40$. The bottom wall section of the domain is obtained symmetrically.

The resulting shape is to represent a cross section of an average uterus with no lesions, fibroids or other malformations. We assume that the catheter is inserted axially at the cervical region. The fluid domain includes the catheter cavity. Thus, we compute the fluid flow in the uterine cavity with only the catheter walls excluded. The catheter in the computations has 2 mm outer and 0.8 mm inner diameter. The uterine cavity domain with catheter inserted is depicted on Fig. 1.

We assume that during the ET procedure the domain representing the internal cavity of the uterus is not changing in time, given that the injected fluid is a small fraction of the uterine fluid. However, if the withdrawal of the catheter is also simulated, the domain for the flow simulation does depend on the time t due to the moving catheter. In general, we consider a time dependent domain Ω_t .

Governing Equations

We assume constant density and viscosity and use the incompressible Navier–Stokes equation as a model for the fluid flow during the ET process. The equations in vector form are given as

$$\frac{\partial \vec{u}}{\partial t} + (\vec{u} \cdot \nabla) \vec{u} + \frac{1}{\rho} \nabla p = \nu \Delta \vec{u},$$

where $\vec{u} : \Omega_t \times [0, t_e] \rightarrow \mathbb{R}^2$ is the velocity field on the time dependent domain Ω_t and the simulated time

horizon $[0, t_e]$, $p : \Omega_t \times [0, t_e] \rightarrow \mathbb{R}$ is the pressure and ρ and ν are the constant density and kinematic viscosity, respectively.

Boundary Conditions

The boundary conditions throughout the domain boundary, including the catheter's tip, inner and outer walls, have been chosen as no-slip and no penetration conditions. The exception from this is the "stem" section of the catheter cavity at the cervix \mathcal{C} , where inflow conditions are specified with prescribed velocity profile. Specifically, with ϕ_t , ϕ_n representing the tangential and normal velocity components at the boundary and $\partial\tilde{\Omega}_t = \partial\Omega_t \setminus \mathcal{C}$,

$$\begin{aligned} \phi_t|_{\partial\tilde{\Omega}_t} &= 0, & \phi_n|_{\partial\tilde{\Omega}_t} &= 0, \\ \phi_t|_{\mathcal{C}} &= f_1(t), & \phi_n|_{\mathcal{C}} &= f_2(t), \end{aligned}$$

where f_1 , f_2 are given functions of time t . For the current simulation study f_1 and f_2 are piecewise constant functions with different values for different stages of the procedure, namely, the injection, rest and catheter withdrawal stages.

Numerical Method

The complex non-linear dynamics was computed using an approximation scheme based on finite differences on a staggered rectangular grid, with the pressure being represented at the center of the rectangular element and the vertical and horizontal velocity components at the center of the right vertical and upper horizontal edge, respectively.¹⁰ The calculations were carried out using fluid elements in the range of 106,000–115,000. The boundary conditions in the code¹⁰ have been extended to accommodate moving boundaries with specified velocities at the catheter withdrawal stage.

Procedural Parameters

In our experiments a simulated embryo transfer starts with the catheter inserted in the uterus and has been divided into a sequence of three consecutive time intervals or stages: the injection, the rest and the withdrawal intervals. We assume that during the injection stage a specified fluid volume, containing the embryo(s), is injected into the uterine cavity from the contents of the catheter at a constant rate or speed. The injection is followed by a rest period (with no injection and no catheter motion) which in turn is followed by the stage in which the catheter is

withdrawn from the uterus, also at a constant speed. Simulations show that the withdrawal causes a back flow in the uterus from the fundal region which may result in carrying the embryo(s) toward the cervix. We can also observe that this back flow can be limited or eliminated if the catheter withdrawal coincides with a secondary injection of some additional fluid that we refer to as withdrawal injection, essentially to fill partially or fully) the volume vacated by the withdrawn catheter. In our parametric study we included the possibility of injecting fluid during the withdrawal stage for partial or full volume replacement to investigate its effect on embryo placement.

We considered 6 parameters in our study of ET, namely, the *injection time* (IT) i.e., the length of the first stage, the *catheter distance* (CD) i.e., the initial distance of the catheter tip from the fundus, the *injected volume* (IV) during the first stage, the *rest time* (RT) i.e., the length of the second stage, the *withdrawal speed* (WS) i.e., the speed at which the catheter is removed in the last stage, and the *volume replacement* (VR) by simultaneous constant rate injection during catheter withdrawal (specified as percentage of the volume vacated by the withdrawal). The dimensions of the parameter values are measured in centimeter, microliter, seconds and centimeter per seconds for the distance, volume, time and speed quantities, respectively. These parameters have been selected as they may be directly controlled during the procedure, other parameter values such as the length of the last stage, the injection speed in the first and injected volume in the last stage can be directly obtained from the values for the selected 6 above. The table below lists the values we used for the 6 parameters in the simulation. These values are realistic considering current clinical practice (Table 1).

The procedure with all combinations of the given values for the 6 parameters are simulated providing $3^6 = 729$ data points covering a rectangular solid region in the 6-dimensional parameter space where a data value is collected at each vertex, inside each edge and face.

The computations have been performed on a 9-node Linux Beowolf cluster with 1.9 MHz Pentium 4 processors at the University of Wisconsin–Milwaukee, Department of Mathematical Sciences. With dedicated usage of this platform and without the implementation of parallelization techniques outlined below the com-

TABLE 1. Parameters values for the ET parameter sensitivity study.

IT (s)	CD (cm)	IV (μl)	RT (s)	WS (cm/s)	VR (%)
0.5	0.5	20	0.5	1.0	0
1.0	1.0	30	5.0	3.0	40
1.5	1.5	40	10.0	5.0	100

putational experiment required over 400 hours of computation time. The large simulation effort was conducted to identify parametric region(s) associated with good embryo placement results (as predicted by simulated fluid flow) in the specified part of parametric space feasible in ET.

Collected Simulation Data and Its Evaluation

The total simulated time duration for the simulated experiments, (including the injection, the rest and the withdrawal stages) is ranging from the minimal 2.18 s to the maximal 18.5 s. Storing the full flow dynamics over the whole simulated time horizon is not feasible. For the validation of the solver we did create a visualization tool that enabled us to view a movie showing the computed velocity field of the flow dynamics and the motion of traced particle sets. To perform the parameter study however, we only needed to trace a limited number of particles that are used to identify the region occupied by the embryos at the end of the run. With this approach storage capacity is not a bottleneck.

We considered placement of an embryo loaded in the catheter 1 cm from its tip. To identify the region reached by the embryo we traced an array of N particles throughout the injection representing N different potential embryo trajectories. For the results presented $N = 7$. Initially the traced particles are spaced equally along the catheter cavity's cross section 1 cm from the tip. (A small change in the particle's initial relative position to the catheter wall results in substantially different particle trajectories.) The position of the particle set at the end of the simulated procedure is used as an estimation for the region occupied by the small injected fluid volume adjacent to the embryo after the procedure, and hence that of the possible position of the embryo itself.

In general terms, the objective of the procedure is to place the embryo in a region close to the fundus while avoiding the entrance of the fallopian tubes (thus to limit the risk of ectopic pregnancy).

To quantify these objectives we formulate a risk function R below. The risk function is composed of three component terms and its minimal values are associated with optimal placement.

Let $\mathbf{P} = (\text{CD}, \text{IT}, \text{IV}, \text{RT}, \text{WS}, \text{VR})$ be a selected parameter array. Let $\mathbf{T}_1, \mathbf{T}_2$ denote the position vectors of the entrance of the two fallopian tubes with distance D_t between them and let $\mathbf{a}_1, \mathbf{a}_2, \dots, \mathbf{a}_N$ be the final locations of the traced particles i.e., the locations at the end of the withdrawal stage of the simulated procedure. Clearly the final locations depend on \mathbf{P} i.e., $\mathbf{a}_i = \mathbf{a}_i(\mathbf{P})$.

We define a quantity associated with the ectopic pregnancy risk as

$$E(\mathbf{P}) = \frac{D_t}{2} \left(\frac{1}{\min_{i=1, \dots, N} |\mathbf{a}_i - \mathbf{T}_1|} + \frac{1}{\min_{i=1, \dots, N} |\mathbf{a}_i - \mathbf{T}_2|} \right),$$

and two quantities associated with the placement region: the standard deviation of the distance of the traced particles to their average location as a measurement of the size of the region reached

$$S(\mathbf{P}) = \sqrt{\sum_{i=1}^N \left| \mathbf{a}_i - \frac{\sum_{j=1}^N \mathbf{a}_j}{N} \right|^2},$$

and the traced particles' mean lateral distance to the fundal wall

$$F(\mathbf{P}) = \frac{1}{N} \sum_{i=1}^N d_f(\mathbf{a}_i),$$

where $d_f(\mathbf{a}_i) = x_i - a_i^1$ with $\mathbf{a}_i = (a_i^1, a_i^2)$ and (x_i, a_i^2) is a corresponding point on the fundus wall. Consider the functions E_n , S_n and F_n defined by normalizing E , S and F to have average 1. (e.g., $E_n = E / \text{Av}_E$, where $\text{Av}_E = \frac{1}{729} \sum_{\mathbf{P}} E(\mathbf{P})$). The risk function $R(\mathbf{P})$ is now defined as a linear combination of E_n , S_n and F_n ,

$$R(\mathbf{P}) = \alpha_E E_n(\mathbf{P}) + \alpha_S S_n(\mathbf{P}) + \alpha_F F_n(\mathbf{P}).$$

The chosen values for the weights α_E , α_S and α_F should reflect the weighting of the impact of the three measurements on the procedure's success. Ideally, they should be determined based on clinical results. In the current study we have chosen the values $\alpha_E = 0.2$, $\alpha_S = 0.3$, $\alpha_F = 0.5$ that reflect the authors' judgment for the defined R to represent an acceptable measure associated with the likely success of the corresponding procedure. This parameter selection is supported by the fact that the conclusions we arrive at, regarding the optimal placement based on our risk model, are generally in line with the conclusions of investigations in the literature that are aimed at determining optimal ET parameter choices based on clinical data. As additional, more detailed clinical data becomes available regarding embryo placement, the risk model we propose needs to be further validated and adjusted.

Efficient Organization of Computations

The availability of a multiprocessor computational platform allows us to reduce computational time required for the data generation for our parameter study. Parallelization can be utilized at the level of the underlying Navier–Stokes code applying domain decomposition and at the parametrization level computing risk values at the selected points in the parameter space. Because each experiment is divided into three stages and the individual stages depend only on a

limited number of parameters as well as the flow conditions at the end of the previous stage we can increase the computational efficiency by sharing common computational tasks among experiments with different parameter sets. In our computational problem, the first stage of the fluid solver depends only on the values of the three parameters IT, CD and IV. This gives 27 different first stage computations shared by the total 729 experimental runs. Each different first stage result is shared by 3 runs among the 81 different results up to the end of the second stage (one additional parameter, RT, influences the second stage) and, in turn, each run up to the end of the second stage is shared by 9 runs in the total of 729 (considering the additional parameters WS and VR). Additionally, the only parameter in the second stage is the simulated time length of the stage, thus the second stage results for all three choices for RT associated with the same first stage result can be obtained from a single run, saving the pressure, velocity and traced particle arrays at different times. This means that by storing the results at the end of the first and second stages and by implementing the option of continuation of stored runs in the fluid code and a scheduler that distributes the computational load among the available processors, we can save considerable computation time. Specifically, 26/27th (about 96%) of all first stage computations and approximately 25% of all second stage computations can be saved (the later percentage depends on the speed of convergence in the fluid solver during the rest stage which in turn depends on the chosen error tolerance and the maximal allowed SOR iteration in each time step¹⁰). For the approach

outlined above the scheduling and communication costs are negligible, but 108 intermediate computational steps should be stored (27 first stage results and 81 second stage results). This storage requirement is not excessive and would carry the benefit of additional computational savings in some cases when the experiment is repeated with partially different parameter values.

On a Beowulf cluster for our problem the concentration of available computational resources on the parametrization level is favored to the parallelization at the level of the fluid solver as the efficiency of the parallelized fluid solver decays considerably with the number of processors (with increasing communication cost) while, as we indicated, the efficiency is effectively constant with the outlined computational approach at the level of parametrization (at least as long as the number of processors is below 27).

RESULTS AND DISCUSSION

Extreme Values of the Risk Function

The obtained values for the risk function R along with its component functions E_n , S_n and F_n , normalized to have average 1, are plotted on Figs. 3–5. The values of R are scaled and shifted on the vertical axis to enhance the viewing by separating the graphs and avoiding “overwriting”.

We remark that to evaluate the results of the parametric study the particular values of these functions are not relevant, only their values relative to other parametric positions.

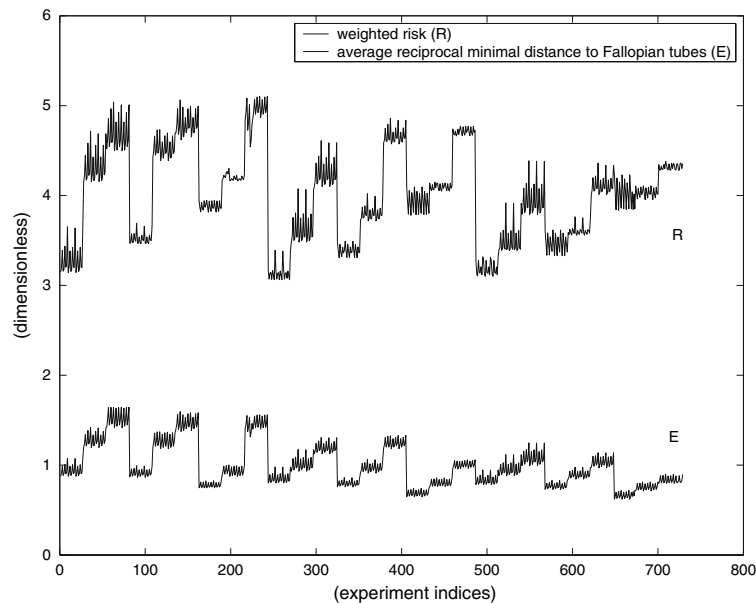


FIGURE 3. The risk function R and its component E_n are plotted on a lexicographical experiment order.

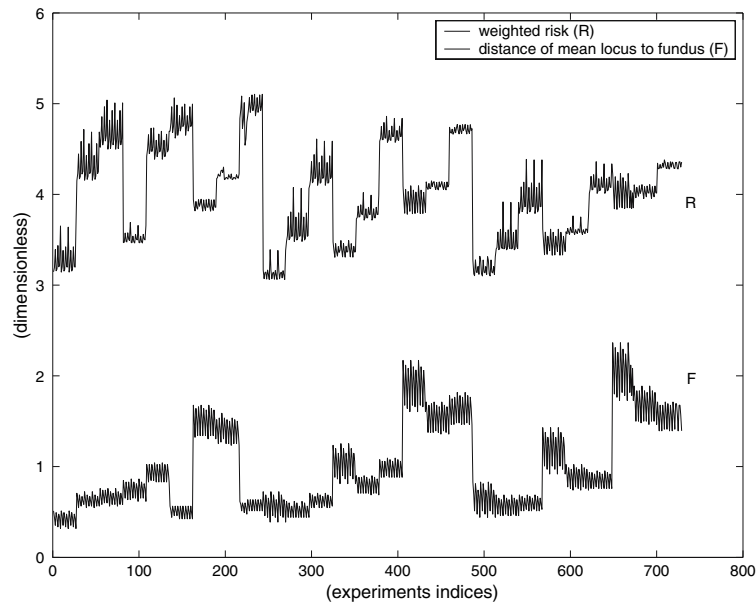


FIGURE 4. The risk function R and its component F_n are plotted on a lexicographical experiment order.

In these plots the values at the points on the 6-dimensional rectangular parametric solid are ordered linearly according to the lexicographical ordering of arrays. In particular, the position of a vector $[u_1, u_2, u_3, u_4, u_5, u_6]$ with entries $u_i(\mathbf{P}) \in \{0,1,2\}$, where 0 represents the low parameter value, 1 the medium and 2 the high value, is associated with the $j(\mathbf{P}) = 1 + \sum_{i=1}^6 3^{6-i}u_i$ position in the linear ordering. (E.g.: $[u_1, u_2, u_3, u_4, u_5, u_6] = [0,0,0,0,0,0]$ corresponds to the 1st parameter combination, $[u_1, u_2, u_3, u_4, u_5, u_6] = [0,1,0,2,0,0]$ corresponds to the

100th and $[u_1, u_2, u_3, u_4, u_5, u_6] = [2,2,2,2,2,2]$ to the 729th parameter combination.) Additionally, on Fig. 6 we plotted R along with the scaled values of the first three parameters IT, CD and IV. The values of these parameters have also been shifted to improve readability and the relevant parameter information can be read as high, medium and low value. Studying this figure helps to clarify visually the lexicographical ordering used on the horizontal axis and to interpret the plots of the risk function and its components.

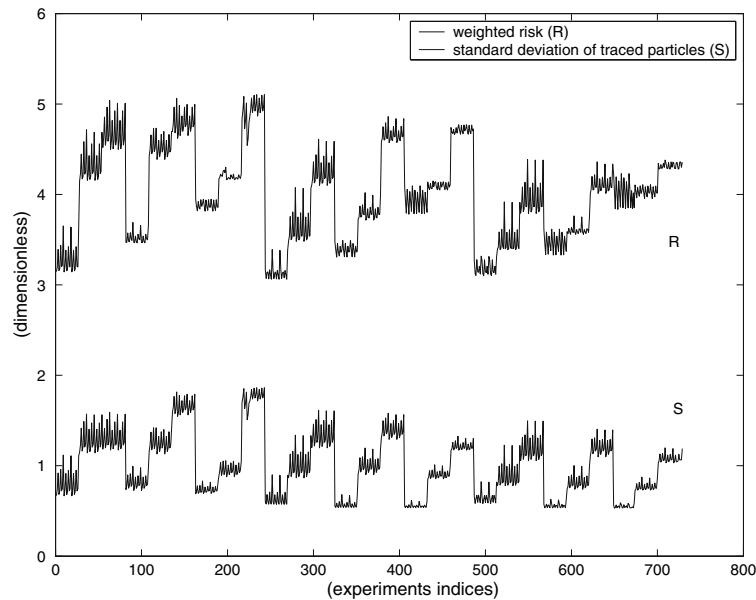


FIGURE 5. The risk function R and its component S_n are plotted on a lexicographical experiment order.

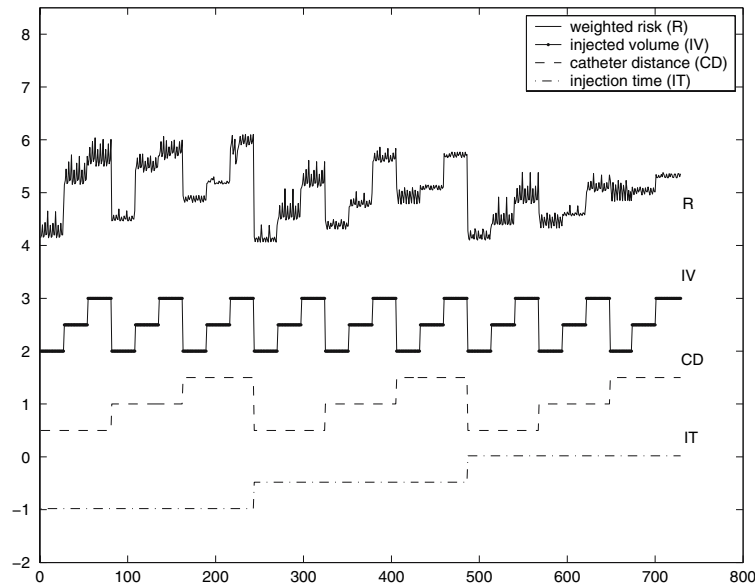


FIGURE 6. Dependence of the risk function R on the parameters IT , CD and IV .

In general, we can conclude based on Figs. 3–6, that IT correlates weakly positively with F and have weak, negative correlation with E , S or R . The variables CD and IV strongly positively correlate with E , S and R .

The desired minimal values of R are obtained in three intervals in the lexicographical ordering of the computational experiments: [1,27] (with corresponding parameter values $IT = 1$, $CD = 0.5$, $IV = 20$), [244, 270] ($IT = 0.5$, $CD = 0.5$, $IV = 20$) and [487,514] ($IT = 1.5$, $CD = 0.5$, $IV = 20$). The low value regions for R are associated with the lowest injected volume and smallest distance of the catheter's tip to the fundus. Furthermore, it is clear from Fig. 6 that each combination of the first 3 parameters determine relatively constant R values with up to 15% oscillations caused by variations of the other three parameters. (The percentage cannot be accurately read from the graphs of R due to the vertical shift we adopted to enhance the viewing.)

The minimal value of R is attained at $j = 260$ and $j = 269$ ($IT = 1$, $CD = 0.5$, $IV = 20$, $RT = 5$ and 10 , $WS = 5$, $VR = 100$). Comparable locally minimal low R values are at $j = 10$, $j = 19$ ($IT = 0.5$, $CD = 0.5$, $IV = 20$, $RT = 5$ and 10 , $WS = 1$, $VR = 0$) and $j = 498$, $j = 507$ ($IT = 1.5$, $CD = 0.5$, $IV = 20$, $RT = 5$ and 10 , $WS = 1$, $VR = 100$). Trajectories of the traced particles from the computational experiments associated with these indices are plotted on Figs. 7–9.

The highest values of R (i.e., maximal risk values) are associated with the experiments with index intervals [55,81] ($IT = 0.5$, $CD = 0.5$, $IV = 40$), [136,162] ($IT = 0.5$, $CD = 1$, $IV = 40$) and [217,243] ($IT =$

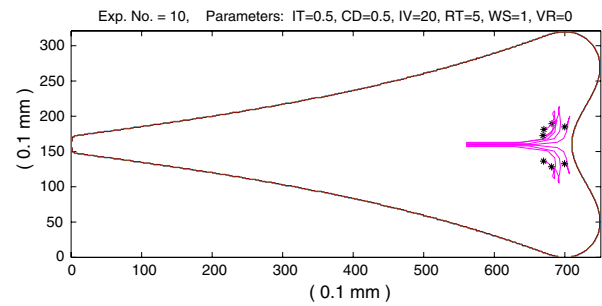


FIGURE 7. Particle traces for experiment No. 10 ($IT = 0.5$, $CD = 0.5$, $IV = 20$, $RT = 5$, $WS = 1$, $VR = 0$).

0.5 , $CD = 1.5$, $IV = 40$), all at highest injected volume ($40 \mu\text{l}$) and shortest injection time (0.5 s), i.e., highest injection velocity. Risk values are also close to maximal in the interval [379,405] ($IT = 1$, $CD = 1$, $IV = 40$). Maximal or locally maximal values are attained at the experiments indexed $j = 63$ ($IT = 0.5$,

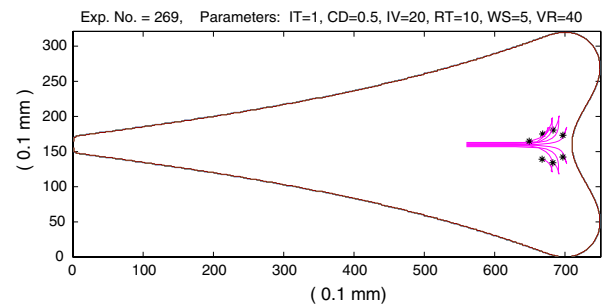


FIGURE 8. Particle traces for experiment No. 269 ($IT = 1$, $CD = 0.5$, $IV = 20$, $RT = 10$, $WS = 5$, $VR = 40$).

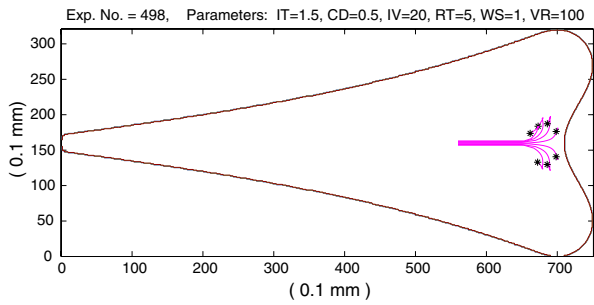


FIGURE 9. Particle traces for experiment No. 498 (IT = 1.5, CD = 0.5, IV = 20, RT = 5, WS = 1, VR = 100).

CD = 0.5, IV = 40, RT = 0.5, WS = 5, VR = 100) $j = 141$ (IT = 0.5, CD = 1, IV = 40, RT = 0.5, WS = 3, VR = 100), $j = 234$ (IT = 0.5, CD = 1.5, IV = 40, RT = 10, WS = 1, VR = 100) and $j = 387$ (IT = 1, CD = 1, IV = 40, RT = 0.5, WS = 5, VR = 100). Trace trajectories from the computational results for these indices are in Figs. 10–13 and can be contrasted to the near optimal injection traces in Figs. 7–9.

We remark that the shape of the risk function and its extreme values depend on the weights α_E , α_S and α_F . Observing E_n and S_n in Figs. 3 and 5 we can see that decreasing the weight α_F would result in the minimum taken at higher indexed subintervals associated with the parameter pair (IV = 20, CD = 1.5). If we excluded the mean distance to fundus component from the risk function completely, ($\alpha_F = 0$) then the minimum would be taken at the parametric region signified by IT = 1.5, CD = 1.5, IV = 20.

Injected Fluid Flow During the Procedure

It is useful to pay particular attention to the best and worst parameter settings listed above. For this purpose we describe the general behavior of the injected fluid during the stages of the procedure in qualitative terms. Though the description we give is based on viewing the dynamics of the simulated fluid flow that is not fully presentable by a limited number of still images, due to limited space in this article we refer to the plotted fluid particle trajectories traced from the selected cross section of the catheter prior to the injection (Figs. 7–14), to support the description. Viewing the injection simulations dynamically shows that at the start of the injection a pair of vortices form off the tip of the catheter around which the injected fluid particles rotate in opposite directions. The emerging vortices are not stationary, they slowly move away from the tip of the catheter to the sides and toward the fundus during injection. When we inject onto an obstacle (like the fundus wall) the circulation around the vortices become elongated with centers

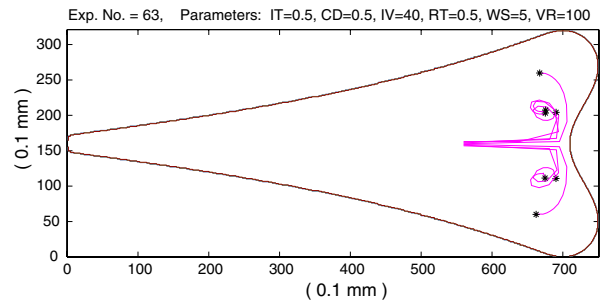


FIGURE 10. Particle traces for experiment No. 63 (IT = 0.5, CD = 0.5, IV = 40, RT = 0.5, WS = 5, VR = 100).

pushed to the sides from the tip. At higher injection speeds the injected fluid particles actually complete the rotation possibly more than once around these moving vortices (as we can see on the particle traces on Figs. 10–12) and the rotation continues for a short time after terminating the injection until the internal friction stops it.

The experiments clearly show that the catheter withdrawal does cause a *back flow* of the injected fluid toward the cervix in the wake of the withdrawn catheter. However, the back flow affects mainly fluid regions close to the catheter wall and tip, and fluid particles farther away from the catheter are less affected by the withdrawal. Fluid particles (and therefore embryos) close to the tip prior to the withdrawal follow the catheter towards the cervix, but at a lower speed than the moving catheter, and as the particles are left behind the effect of the back flow on them quickly diminishes. The speed of the withdrawal itself has little effect on the position change of the traced particles caused by the withdrawal.

Because we noted the back flow and the relative displacement of the particles, we included the parameter VR in the investigation. This was guided by the idea that the injection of additional fluid (intended as “volume replacement”) during the withdrawal could help to control the placement by limiting the back flow. This hypothesis is confirmed by the experimental

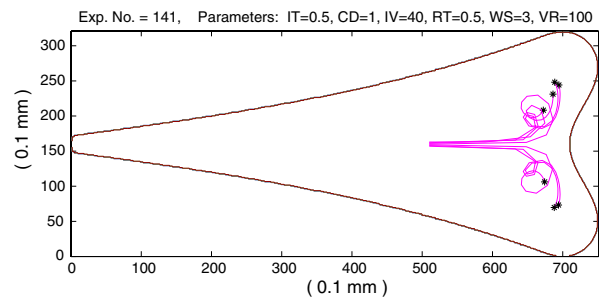


FIGURE 11. Particle traces for experiment No. 141 (IT = 0.5, CD = 1, IV = 40, RT = 0.5, WS = 3, VR = 100).

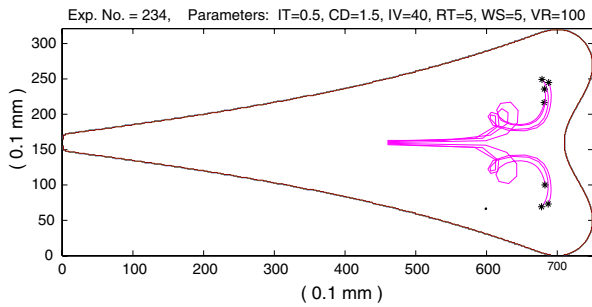


FIGURE 12. Particle traces for experiment No. 234 ($IT = 0.5$, $CD = 1.5$, $IV = 40$, $RT = 5$, $WS = 5$, $VR = 100$).

results, showing that the new parameter VR is useful in controlling the value of the risk function.

The Effect of Parameters IT , CD and IV

We remarked that the index intervals with close to minimal value of R are determined by the value of the first three parameters, especially CD and IV . Specifically, $CD = 0.5$ and $IV = 20$ identify the parameter regions of low R value. The combination $IT = 1$, $CD = 0.5$ and $IV = 20$ identifies the optimal choice as measured by the risk function R . This translates to injecting the embryo at medium speed, in a low volume and with the catheter tip close to the fundus. We can observe on Fig. 6 that the risk profile of the procedure is deteriorating with increasing values of both CD and IV , independently of each other. Increasing the injection time (thereby decreasing its speed) on average also improves the risk profile, though less dramatically. These results are in line with the published clinical studies on the impact of these parameters' variations on successful embryo implantation. This validates our choice of combination of 2D fluid dynamics injection model and the risk model represented by R to predict the success of implantation.

As we can observe on Figs. 7–9, low volume injection results in the traced particles being located in a compact group close to the catheter tip at the end of

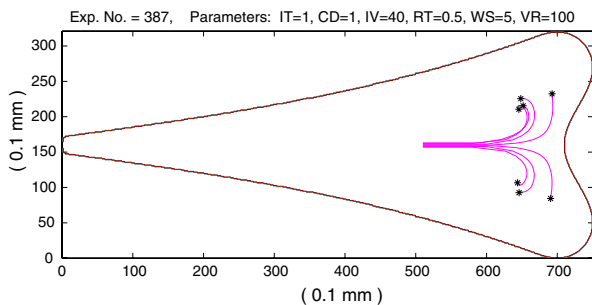


FIGURE 13. Particle traces for experiment No. 387 ($IT = 1$, $CD = 1$, $IV = 40$, $RT = 0.5$, $WS = 5$, $VR = 100$).

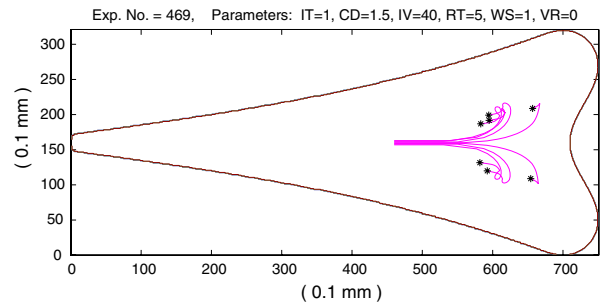


FIGURE 14. Particle traces for experiment No. 469 ($IT = 1$, $CD = 1.5$, $IV = 40$, $RT = 5$, $WS = 1$, $VR = 0$).

the first stage of the procedure. It also limits the particle motion in the second stage by reducing the rotation around the off-tip vortices. With low catheter distance this compact fluid portion is located close to the fundus. As we outline below in the discussion on the effect of catheter withdrawal and the volume replacement, by controlling the back flow generated during the third stage we can prevent the translation of the embryo toward the cervix.

The Effect of Parameters RT , WS and VR

Next we turn our attention to the effects of the last 3 parameters. We considered fixed values for the parameters IT , CD and IV , determining a group of 27 experiments (corresponding to consecutive intervals of length 27 in the lexicographical order), and investigated the impact of varying the values of the parameters RT , WS and VR on the value of R . Figures 15 and 16 depict the values of the parameters RT , WS and VR versus R for selected experiment groups (all values are scaled and shifted along the vertical axis to improve readability of the graph).

The experiments show that varying the WS has essentially no effect on the traced particle trajectories (hence on the values of R).

Additionally, varying the values of the rest time parameter RT does not have a significant effect on the values of the risk function R . (In particular RT has not affected the lowest value regions of R .) The exception from this rule appeared in our series of experiments with the lowest injection time ($IT = 0.5$) i.e. fastest injection speed along with the largest catheter distance ($CD = 1.5$). We can observe the effect of these instances in the “kinks” on R on Fig. 6 in the index ranges [190,216] and [217,243]. In the experiments with short rest times the positions of the injected particles relative to catheter tip do depend on RT , as the particles still rotate in the apical vortices. The particle position at the start of the withdrawal is important, as particles in proximity to the catheter tip will be more

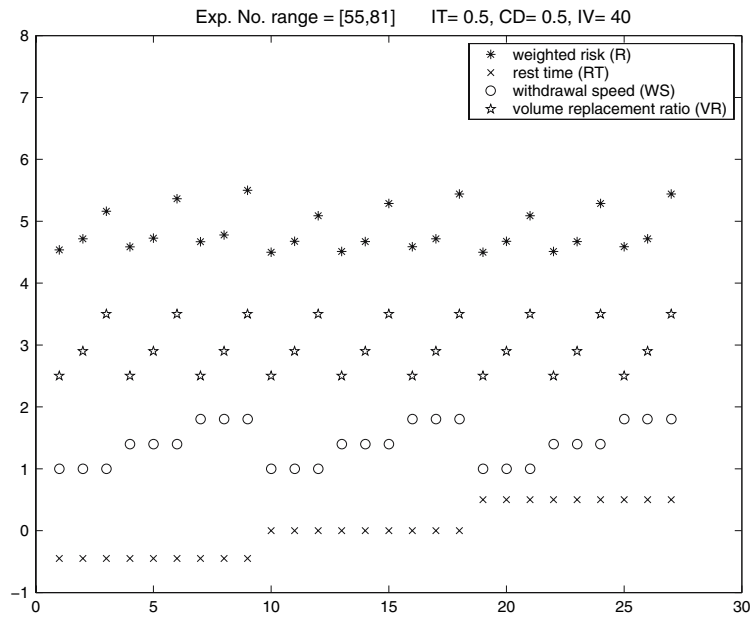


FIGURE 15. Dependence of the risk function R on the parameters RT, WS and VR with fixed IT = 0.5, CD = 0.5 and IV = 40 values.

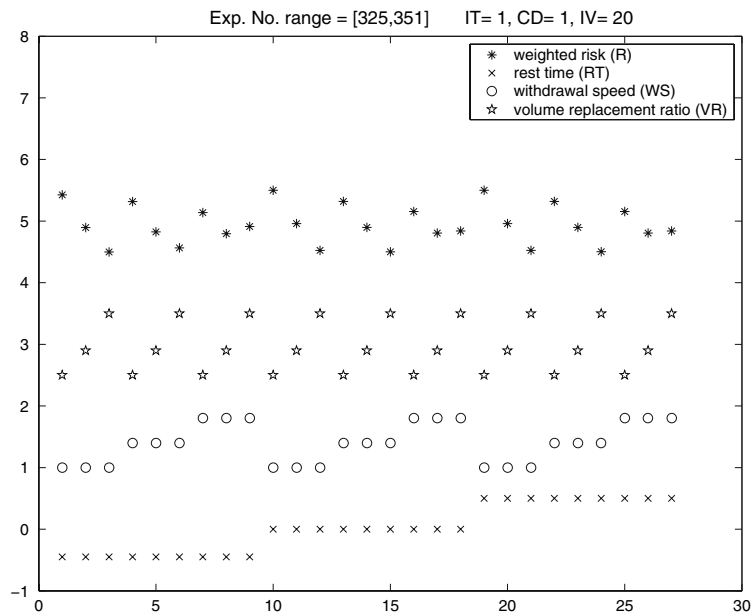


FIGURE 16. Dependence of the risk function R on the parameters RT, WS and VR with fixed IT = 1, CD = 1 and IV = 20 values.

affected by the back flow than more distant particles. In summary, RT has a non-linear effect on R in the small value ranges but the dependence vanishes for larger RT values as the fluid stops rotating.

The simulated experiments also show that there is no overall correlation between the risk value R and the parameter values of the catheter withdrawal speed WS and replacement ratio VR. The effects are more subtle and dependent on the other variables as well. Compared to no volume replacement (VR = 0) partial

volume replacement (VR = 40) limits the particle motion caused by the withdrawal of the catheter and full volume replacement (VR = 100) mostly eliminates it. It is interesting to note that the back flow has a dual effect on the particles' spread: the particles' motion toward the withdrawn tip retracts them away from the fundus, as expected, but it may also reduce the spread of the particles. Depending on the position of the particles at the onset of withdrawal the weighting of these two effects on R is different. We wish to

emphasize that in our experiments withdrawing the catheter has not shown the risk of removing the embryo from the uterus as no particle was removed or moved markedly close to the cervix.

Increasing the particles' distance from the fundus results in increasing the F component of the risk function R , while contracting their spread is associated with decreasing the E and S components. If at the beginning of the withdrawal the particles are in a compact area (that can be best obtained by injection of a small volume) then, with no volume replacement, the withdrawal has little effect on the spread, more on the particles' distance to the fundus increasing the value of F and thus the value of R . Volume replacement prevents this increment in R and thus, is effective in such situations. In particular, this is the case for the parameter regions that minimize the value of R . (The exception from this is the case where the low volume is injected close to the fundus at the highest injection speed.)

On the other hand, if in the no volume replacement case at the beginning of the withdrawal the particles are more spread apart (after higher volume/more aggressive injection or by injecting from close to the fundus) then the effect of the withdrawal on the spread is more significant, resulting in a decrease in R . Since volume replacement prevents this, it effectively increases the value of the risk function.

In summary, we conclude that the use of volume replacement has a reinforcing effect on the risk as measured by R : both deteriorating the results for the worst performing parameter settings and enhancing the results for the best performing parameter settings. One exception from this rule is represented by the case where the low volume is injected close to the uterine fundus at the highest injection speed. In this scenario the traced particles are pushed away from the catheter's tip and spread close to the fundus walls. In this case it is exactly the withdrawal generated back flow that pulls the particles into a more compact set situated close to the fundus with corresponding lower R value.

CONCLUSIONS

Though to implement full control of the embryo transfer procedural parameters is technologically not difficult, in the current practice few of the parameter values can be controlled tightly. Our parametric study shows that in ET there is a complex dependence of fluid placement on the studied procedural parameters. The results of our simulations generally coincide with available clinical studies on the effect of the parameters on ET success rate. Additionally, we computationally investigated the effect of a novel procedural element,

the volume replacement, and found that its introduction into the procedure can potentially improve the placement results. As an extension of this work, additional parameters representing variations of the uterine anatomy may be considered and the parameter study we performed may be refined in the identified low risk parameter regions.

It is clear that embryo implantation after ET is a complex physiological phenomenon. Our model is only based on simplified uterine anatomy and fluid propagation in the uterus. Other issues, such as damage to the endometrium secondary to trauma caused by the catheter, may have an impact on the success of ET and need to be better understood. Consideration of the individual uterine anatomy and better understanding of the physiology of embryo implantation may ultimately lead to individualized transfer methods for every particular patient. New insights into the implantation process could be used to improve the risk model we introduced.

We envision that fluid simulations coupled with the use of imaging techniques will have the potential to provide a basis for future personalized ET procedures, in particular taking into account individual factors such as the size and shape of the uterine cavity.

ACKNOWLEDGMENT

The authors are grateful to Professor Albert Milani for his interest, suggestions and encouragements.

REFERENCES

- ¹Allen, W. R., C. A. Butler, and M. R. Mackley. Rheological characterization of estrous uterine fluid in the mare. *Theriogenology* 58:503–506, 2002.
- ²Baba, K., O. Ishihara, N. Hayashi, M. Saitoh, J. Taya, and K. Kinoshita. Where does the embryo implant after embryo transfer in humans? *Fertil. Steril.* 73:123–125, 2000.
- ³Bilalis, D., S. A. Marangou, N. Polidoropoulos, P. Sissi, M. Argyrou, S. Doriza, S. Davies, A. Antonakopoulos, and M. Mastrominas. Use of different loading techniques for embryo transfer increasing the risk of ectopic pregnancy. *Human Reprod.* (Abstract Book, P-479), 17, 162, 2002.
- ⁴Ebner, T., C. Yaman, M. Moser, M. Sommergruber, W. Polz, and G. Tews. The ineffective loading process of the embryo transfer catheters alters implantation and pregnancy rates. *Fertil. Steril.* 76:630–632, 2001.
- ⁵Eytan, O., D. Elad, U. Zaretsky, and A. J. Jaffa. A glance into the uterus during in vitro simulation. *Human Reprod.* 19:562–569, 2004.
- ⁶Fauci, L. J. and R. Dillon. Fluid mechanics of reproduction. *Annu. Rev. Fluid Mech.* 38:371–394, 2006.
- ⁷Griebel, M., T. Dornseifer, and T. Neunhoeffer. Numerical Simulation in Fluid Dynamics, A Practical Approach. Society for Industrial and Applied Mathematics Press, Philadelphia, 1998.

- ⁸Kovacs, G. T. What factors are important for successful embryo transfer after in vitro fertilization?. *Human Reprod.* 14:590–592, 1999.
- ⁹Lozeau, A. M., and B. Potter. Diagnosis and management of ectopic pregnancy. *Am. Fam. Physician* 72:1707–1714, 2005.
- ¹⁰Meldrum, D. R., R. Chetkowski, K. A. Steingold, D. de Ziegler, M. H. Cedras, and M. Hamilton. Evolution of a highly successful in vitro fertilization – embryo transfer program. *Fertil. Steril.* 48:86–93, 1987.
- ¹¹Schoolcraft, W. B., E. S. Surrey, and D. K. Gardner. Embryo transfer: technics and variables affecting success. *Fertil. Steril.* 76:863–870, 2001.
- ¹²Yaniv, S., D. Elad, A. J. Jaffa, and O. Eytan. Biofluid aspects of embryo transfer. *Ann. Biomed. Eng.* 31:1255–1262, 2003.